

Quotient Quiver Subtraction – Classical Groups

Sam Bennett, Amihay Hanany, Guhesh Kumaran

*Abdus Salam Centre for Theoretical Physics, Imperial College London,
Prince Consort Road London, SW7 2AZ, UK*

E-mail: samuel.bennett18@imperial.ac.uk, amihay.hanany@imperial.ac.uk,
guhesh.kumaran18@imperial.ac.uk

ABSTRACT: Quotient quiver subtraction is a simple combinatorial prescription for gauging Coulomb branch isometry subgroups of 3d $\mathcal{N} = 4$ quiver gauge theories. This paper uses Type IIB brane constructions with O5 planes to extend the prescription to gauge $\mathrm{Sp}(n)$, $\mathrm{SO}(n)$, and $\mathrm{Sp}(n)$ coupled to a half-hypermultiplet Coulomb branch isometry subgroups of quivers with unitary gauge groups. The gauging procedure is no longer solely a subtraction – additional steps change the graph type. The method is applied to provide alternative constructions of the Higgs branch of certain SCFTs in higher dimensions.

Contents

1	Introduction	1
2	Type IIB Brane Systems	2
2.1	Reading quivers from brane systems	3
3	Weyl Integration	3
4	$\mathrm{Sp}(n)$ Quotient Quivers	4
4.1	$\overline{\min.E_8} // \mathrm{Sp}(2)$	6
4.2	$(\overline{\min.E_6} \times \mathbb{H}^{12}) // \mathrm{Sp}(2)$	8
5	$\mathrm{SO}(2n)$ Quotient Quivers	12
5.1	$\overline{\min.F_4} // \mathrm{SO}(2)$	14
5.2	$\overline{\min.E_7} // \mathrm{SO}(4)$	15
5.3	$\overline{\min.E_8} // \mathrm{SO}(4)$	16
6	$\mathrm{SO}(2n + 1)$ Quotient Quivers	17
6.1	$\overline{\min.E_6} // \mathrm{SO}(3)$	19
6.2	$\overline{\min.F_4} // \mathrm{SO}(3)$	20
7	$\mathrm{Sp}(n) + \frac{1}{2}\mathbf{F}$ Quotient Quivers	21
7.1	$(\overline{\min.E_6} \times \mathbb{H}) // \mathrm{Sp}(1)$	23
7.2	$(\overline{\min.E_7} \times \mathbb{H}^2) // \mathrm{Sp}(2)$	24
8	Outlook	25

1 Introduction

This paper expands on the concept of *quotient quiver subtraction* [1–3], which translates the question of gauging IR Coulomb branch isometry subgroups of a 3d $\mathcal{N} = 4$ quiver into a straightforward procedure. Importantly, the algorithm bypasses complications from strongly coupled and non-perturbative physics that arise in the IR; as such, Coulomb branch gauging becomes, for a large class of theories, as simple to perform as flavour gauging. Gauging global symmetries and identifying obstructions to their gauging, is a classic problem in physics and identifying convenient ways to do this is tied to the heart of studying gauge theories.

In many cases the gauging of a Coulomb branch isometry subgroup of a theory is equivalent to the flavour symmetry gauging of the same subgroup of a 3d mirror theory [4]. Quotient quiver subtraction and other methods for gauging Coulomb branch isometry subgroups [5, 6] are able to go beyond since there are many moduli spaces which do not admit known descriptions as a Higgs branch hyper-Kähler quotient [7] but instead as a moduli space of dressed monopole operators or also as dressed instanton

operators [8, 9]. Examples include the moduli space of exceptional group instantons on \mathbb{C}^2 which have descriptions as a Coulomb branch where Higgs branch descriptions are unknown [10].

A broader class of these moduli spaces are Higgs branches of theories with eight supercharges in four, five and six dimensions [11–18]. In these theories there may be certain phases where additional massless states arise which may not have a perturbative or even a Lagrangian description. To bypass this, the notion of magnetic quivers provides a description of these Higgs branches as a moduli space of monopole operators. Flavour symmetry gauging in these theories with eight supercharges may be described by quotient quiver subtraction or related operations on the magnetic quiver. This motivates the discovery of combinatorial operations on $3d \mathcal{N} = 4$ quivers, such as quotient quiver subtraction, as they may be directly used to study non-trivial physics in other dimensions.

Quotient quiver subtraction algorithms have been used so far to gauge $SU(n)$ Coulomb branch global symmetry subgroups of unitary quiver theories [1], $SO(n)$ and $Sp(n)$ subgroups of framed orthosymplectic quivers [3], and $SU(2)$, $SU(3)$, G_2 , and $SO(7)$ subgroups of unframed orthosymplectic quivers [2]. This list is extended here to gauging $Sp(n)$, $SO(n)$, and $Sp(n)$ coupled to a half-hypermultiplet Coulomb branch global symmetry subgroups, using Type IIB brane systems with O5 planes and their mirror the ON. The resulting algorithms involve changing the graph type to that of Dynkin type D or type C for $Sp(n)$ and $SO(n)$ respectively.

The prescription for quotient quiver subtraction, much like previous quotient quiver subtraction and quiver polymerisation algorithms, applies to quivers with a long enough leg of gauge nodes going from $U(1) - U(2) - \dots$ which supports the symmetry being gauged. Furthermore it deals only with cases with *complete Higgsing* of the symmetry being gauged.

The $Sp(n)$ and $SO(n)$ quotient quiver subtraction are used to provide alternative checks of certain $4d \mathcal{N} = 2$ dualities in [19], with a more direct approach to deriving magnetic quivers. Further examples provide new relationships between the Higgs branches of certain rank-1 $4d \mathcal{N} = 2$ theories under gauging.

Organisation of the paper. The Type IIB brane systems and notations used throughout this paper are reviewed in Section 2. The concept of Weyl integration is introduced in Section 3 which will be the main computational check of the quotient quiver subtraction algorithms. Section 4 introduces the quotient quiver subtraction process for $Sp(n)$ groups, Sections 5 and 6 repeat the process for $SO(2n)$ and $SO(2n + 1)$ groups respectively. The case of gauging an $Sp(n)$ with the addition of a half hypermultiplet is done in Section 7. Future directions are discussed in Section 8.

2 Type IIB Brane Systems

The Type IIB brane systems used throughout this paper are the Hanany-Witten [20] brane systems with D3, D5, NS5 brane systems in the presence of O5 and ON planes. The spacetime occupation of branes and orientifold planes are summarised in Table 1.

	x^0	x^1	x^2	x^3	x^4	x^5	x^6	x^7	x^8	x^9
NS5/ON	✓	✓	✓	✓	✓	✓				
D5/O5	✓	✓	✓					✓	✓	✓
D3	✓	✓	✓				✓			

Table 1: Occupation of NS5, D5, and D3 branes in spacetime for Hanany-Witten setup.

In terms of the brane diagrams, D3 branes will be denoted by horizontal lines, D5 and O5 will be denoted by crosses and unfilled circles respectively, whilst NS5 and ON will be denoted by vertical solid lines and dashed lines respectively.

2.1 Reading quivers from brane systems

The rules for reading off quivers from brane systems in the presence of O5 or ON planes follows those established in [20–23] but it is worth reviewing them once more. A stack of n D3 branes suspended between two NS5 branes gives rise to an electric $U(n)$ vector multiplet, in quiver notation this will be denoted by an unfilled circle with label n . If there are also k D5 branes in this NS5 brane interval, there is a contribution of k bifundamental hypermultiplets with flavour symmetry $U(k)$. The flavours are denoted with a box with label k and the bifundamental hypermultiplets are denoted with an edge. These rules receive a slight modification in the presence of O5 or ON planes.

Firstly when $2n$ D3 branes pass through an $O5^-$ plane, the gauge theory on the D3 worldvolume is an $Sp(n)$ gauge theory. Similarly, when $2n$ D3 branes end on an $O5^+$ plane, there is an $SO(2n)$ gauge theory on the D3 worldvolume. In the presence of an $\widetilde{O5^+}$, the theory on a stack of $2n + 1$ D3 is $SO(2n + 1)$ gauge theory. The last case is when $2n$ D3 branes pass through an $\widetilde{O5^-}$, in which case the resulting gauge theory is $Sp(n)$ with a half-hypermultiplet.

In the case of ON planes which are S-dual to the O5 planes of corresponding type, the type of gauge symmetry remains unitary but the graph shape of the quiver changes forming a Dynkin diagram shape. When n D3 branes pass through ON^- , one chooses a partition of n into l and $n - l$ (where $n > l$), and the resulting quiver has a bifurcation of $U(l)$ and $U(n - l)$ gauge nodes. The quiver forms a D-type Dynkin diagram shape. In the presence of ON^+ and $\widetilde{ON^+}$, n D3 branes, where n is even and odd respectively, give rise to a non-simply laced edge of multiplicity two with $U(n)$ being the long side. The quiver forms a Dynkin diagram shape of C-type. Finally, when $2n$ D3 end on an $\widetilde{ON^-}$ the quiver forms a Dynkin diagram shape of B-type, with a short $U(n)$ gauge node with non-simple lacing of multiplicity two.

3 Weyl Integration

The effect of gauging global symmetry subgroups on a moduli space \mathcal{M} can be seen through its refined Hilbert series by performing Weyl integration. Suppose \mathcal{M} has global symmetry $G_{\mathcal{M}}$ and refined Hilbert series $HS[\mathcal{M}](t; u_1, \dots, u_{\text{rank}(G_{\mathcal{M}})})$, where t and u_i are fugacities for conformal dimension and global symmetries respectively. Throughout this paper \mathcal{M} will be a Coulomb branch (or moduli space of dressed monopole operators) so this Hilbert series may be computed with the monopole formula [24] or via Hall-Littlewood methods [25, 26]. Gauging a subgroup G , where $G \times G' \subset G_{\mathcal{M}}$ (with G' being the commutant of G inside $G_{\mathcal{M}}$), corresponds to a Weyl integration on $HS[\mathcal{M}]$ as shown in (3.1).

$$HS[\mathcal{M}///G](t; x_1, \dots, x_r) = \oint_G d\mu_G \frac{HS[\mathcal{M}](t; x_1, \dots, x_r, y_1, \dots, y_{\text{rank}(G)})}{PE[\chi_{\text{Adj}}^G(y_1, \dots, y_{\text{rank}(G)})t^2]}, \quad (3.1)$$

Note that x_i are fugacities for the ungauged symmetry subgroup G' of rank r , and the y_i are fugacities for the gauged symmetry subgroup G .

The equation (3.1) has a simple physical interpretation. The plethystic exponential in the denominator gives symmetrisations of the adjoint representation of G graded by t^2 , which have the

interpretation of imposing additional F-terms that arise when G is gauged [27, 28]. If G is gauged with complete Higgsing (which is assumed and is the case throughout), the F^b -space is a complete intersection and so the (quaternionic) dimension of \mathcal{M} reduces by $\dim G$. This change in dimension hence provides a simple check of complete Higgsing.

4 $\mathrm{Sp}(n)$ Quotient Quivers

An extension of the unitary Coulomb branch gauging algorithm given in [1] involves classical Lie groups of BCD -type. In the following derivation, the logic of appealing to the mirror-theory is made clear, alongside its underpinning in brane systems.

$$(4.1)$$

Consider the $U(N)$ SQCD with $2N + k$ flavours in the left hand side of (4.1). Gauging an $\mathrm{Sp}(n)$ subgroup of the flavour symmetry returns the theory \mathcal{Q}_{1a} in Figure 1a with Type IIB brane system realisation in Figure 1b. The 3d mirror theory of \mathcal{Q}_{1a} is \mathcal{Q}_{1c} drawn in Figure 1c. The corresponding S-dual brane system is given in Figure 1d. Comparing Figure 1c to the quiver in the right hand side of (4.1) leads to a candidate for the quotient quiver, given in (4.2). Figure 1c also shows that a second operation, here termed “splitting”, is necessary in order to correctly realise the gauging. Morally, this is the effect of an ON^0 plane. Note that the total rank of the quotient quiver (4.2) is $n(2n + 1)$, equal to the dimension of $\mathrm{Sp}(n)$ – the splitting operation does not change the rank of the theory. Note also that rebalancing with an additional $U(1)$ gauge node is not required for $\mathrm{Sp}(n)$ gauging.

$$(4.2)$$

Formal Statement of the Rule The $\mathrm{Sp}(n)$ quotient quiver subtraction procedure gauges an $\mathrm{Sp}(n)$ subgroup of the Coulomb branch symmetry of any generic, framed or unframed unitary target quiver. The precise rules are given below.

1. Take a target quiver with a long leg of gauge nodes up to at least $U(2n)$ and at least one more non-negatively balanced gauge node, denoted $U(j)$. The edge in teal denotes some generic connection to the rest of the quiver Q , the only restriction is that the long leg must correspond to long roots of the Coulomb branch global symmetry algebra.

$$(4.3)$$

2. Align the $\mathrm{Sp}(n)$ quotient quiver against the leg of the target quiver and subtract the ranks of the quotient quiver from those of the target. This deletes the gauge nodes from $U(1)$ up to $U(2n)$

Comments Note that the case of $\mathrm{Sp}(1)$ quotient quiver subtraction precisely matches that of the $\mathrm{SU}(2)$ quotient quiver subtraction [1]. Note also that the $\mathrm{Sp}(n)$ quotient quiver is “half” of the $\mathrm{SU}(2n)$ quotient quiver, indicating the \mathbb{Z}_2 which relates the two groups.

The change in the Higgs branch dimension after performing $\mathrm{Sp}(n)$ quotient quiver subtraction is

$$\begin{aligned} \Delta \dim \mathcal{H} &= [-n^2 - (n+1)^2] - \left[\sum_{i=1}^{2n} i(i+1) - \sum_{i=1}^{2n+1} i^2 \right] \\ &= n = \mathrm{Rk}(\mathrm{Sp}(n)) \end{aligned} \quad (4.6)$$

which is precisely the expected increase in Higgs branch dimension.

The $\mathrm{Sp}(n)$ quotient quiver subtraction requires a long leg of gauge nodes of the form $(1) - (2) - \dots - (2n) - (j) -$ where the $\mathrm{U}(2n)$ and $\mathrm{U}(j)$ nodes do not have to be balanced. Such a tail has at least $2n - 1$ balanced gauge nodes contributing at least $\mathrm{SU}(2n)$ Coulomb branch global symmetry. The $\mathrm{Sp}(n)$ is embedded inside this $\mathrm{SU}(2n)$ as

$$[1, 0, \dots, 0, 1]_{\mathrm{SU}(2n)} \rightarrow [2, 0, \dots, 0]_{\mathrm{Sp}(n)} + [0, 1, 0, \dots, 0]_{\mathrm{Sp}(n)} \quad (4.7)$$

This explains the origin of the $\mathrm{Sp}(n)$ symmetry that appears in the long leg. There may be an overall enhancement of the Coulomb branch global symmetry in the starting quiver, in which case the $\mathrm{Sp}(n)$ symmetry being gauged may admit an embedding directly into the enhanced global symmetry. Nevertheless, the $\mathrm{Sp}(n)$ symmetry should be thought of as sourced by the long leg of gauge nodes.

As mentioned, $\mathrm{Sp}(1)$ quotient quiver subtraction is identical to $\mathrm{SU}(2)$ quotient quiver subtraction, with many examples contained within [1]. Non-trivial examples of the algorithm begin with $\mathrm{Sp}(2)$, which requires a quiver with a maximal chain up to $\mathrm{U}(4)$ and at least one more non-negatively balanced gauge node.

4.1 $\overline{\min.E_8} // \mathrm{Sp}(2)$

Consider $\mathrm{Sp}(2)$ quotient quiver subtraction on the affine $E_8^{(1)}$ quiver, shown in two steps in Figure 2. The resulting theory is \mathcal{Q}_2 , with unrefined Coulomb branch Hilbert series given as

$$\mathrm{HS}[\mathcal{C}(\mathcal{Q}_2)] = \frac{\begin{pmatrix} 1 + 36t^2 + 812t^4 + 12735t^6 + 150112t^8 + 1375706t^{10} + 10079822t^{12} + 60251599t^{14} \\ + 298785809t^{16} + 1245721768t^{18} + 4415307757t^{20} + 13424410658t^{22} + 35275096941t^{24} \\ + 80598415736t^{26} + 160929609663t^{28} + 281921275764t^{30} + 434675562921t^{32} \\ + 591245656950t^{34} + 710641440658t^{36} + 755494093072t^{38} + \dots + t^{76} \end{pmatrix}}{(1-t^2)^{19}(1-t^4)^{19}} \quad (4.8)$$

which does not illuminate the identity of the moduli space as a symplectic singularity but does identify the Coulomb branch global symmetry as $\mathrm{SO}(11)$ [29]. This is further verified with the computation of the Coulomb branch and Higgs branch Hasse diagrams [30–33] in Figure 3. From the Coulomb branch Hasse diagram Figure 3a it is clear that the Hasse diagram for the moduli space of 2 $\mathrm{SO}(8)$ instantons on \mathbb{C}^2 is a subdiagram. The bottom two slices form the Hasse diagram of $\overline{n.\min.B_5}$. From the Higgs branch Hasse diagram, in Figure 3b, the Namikawa-Weyl group is seen to be $\mathbb{Z}_2^5 \rtimes S_5$. Additionally, the diamond at the bottom is the Hasse diagram of $\mathrm{Sym}^2(D_4)$.

The explicit Hilbert series of the hyper-Kähler quotient may be computed with Weyl integration

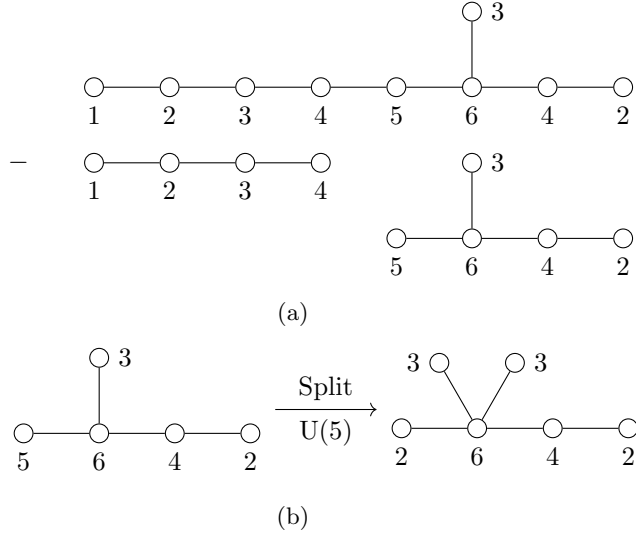


Figure 2: $\text{Sp}(2)$ quotient quiver subtraction on the affine $E_8^{(1)}$ quiver which occurs in two steps. The first step is shown in 2a and involves the subtraction of the $\text{Sp}(2)$ quotient quiver from the maximal leg. The second step, shown 2b, is the splitting of the $\text{U}(5)$ node into a $\text{U}(2)$ and $\text{U}(3)$, producing the resulting quiver \mathcal{Q}_2 . Note the emergence of an S_2 outer automorphism between the two $\text{U}(3)$ gauge nodes.

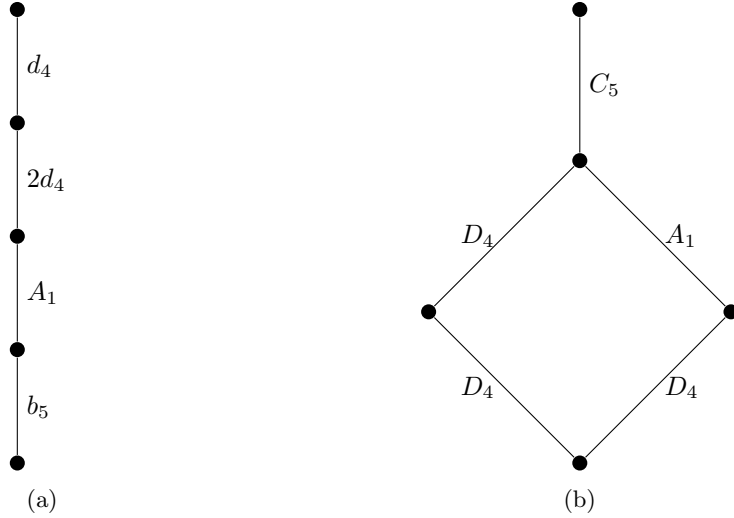


Figure 3: Hasse diagrams for the Coulomb and Higgs branches of \mathcal{Q}_2 in Figure 3a and Figure 3b respectively. The Coulomb branch undergoes a symmetry enhancement to $\text{SO}(11)$, as predicted by [29].

with the following embedding $E_8 \hookrightarrow \text{SO}(11) \times \text{Sp}(2)$ which decomposes the adjoint as

$$(\mu_7)_{E_8} \rightarrow \mu_2 + \nu_1^2 + \mu_1\nu_2 + \mu_5\nu_1 \quad (4.9)$$

where the $\mu_{1,2,3,4,5}$ and $\nu_{1,2}$ are highest weight fugacities for $\text{SO}(11)$ and $\text{Sp}(2)$ respectively.

The result from Weyl integration confirms that

$$\overline{\text{min.}E_8} // \text{Sp}(2) = \mathcal{C}(\mathcal{Q}_2) \quad (4.10)$$

This construction is a realisation of the proposed duality of certain $4d \mathcal{N} = 2$ theories in [19, Table 2 Ex. 1] through magnetic quivers. The pertinent example here is that of the $\text{Sp}(2)$ flavour symmetry gauging of the rank 1 E_8 SCFT [34–37] being dual to the following quiver $\mathcal{Q}_{4.11}$

$$\begin{array}{c}
 \text{SO}(11) \\
 \blacksquare \\
 | \\
 \bullet \\
 \text{Sp}(3) \quad \text{O}(1) \\
 \blacksquare
 \end{array}
 \quad (4.11)$$

where the red edge denotes a “bi-spinor”. In [19, Table 2] this theory is given as $\text{Sp}(3)$ with $\mathbf{14} \oplus 11 \cdot \mathbf{6}$. The $11 \cdot \mathbf{6}$ unambiguously refers to the 11 half-hypers. However, there are two 14-dimensional representations of $\text{Sp}(3)$, the anti-symmetric, $[0, 1, 0]$, and “spinor”, $[0, 0, 1]$ (with the condition that the highest anti-symmetric representation of $\text{Sp}(n)$ is called the spinor). Cancellation of the Witten anomaly [38] requires the total Dynkin index of the matter representations to be an integer. The eleven half-hypers each contribute $T([1, 0, 0]) = 1/2$, the Dynkin index of the spinor is $T([0, 0, 1]) = 5/2$ which gives the desired cancellation, whereas the Dynkin index for the anti-symmetric is $T([0, 1, 0]) = 2$ which does not give the required cancellation. Furthermore, the continuous commutant of $\text{Sp}(2)$ inside E_8 is $\text{SO}(11)$. The spinor is a pseudoreal representation meaning that there is an additional discrete $\text{O}(1)$ flavour symmetry. The anti-symmetric representation is real meaning that there would be an additional $\text{Sp}(1)$ flavour symmetry which does not fit with the embedding of $\text{Sp}(2)$ inside E_8 .

For the purposes of this work, where the focus lies on magnetic quivers, the duality proposed in [19] suggests that the Coulomb branch of \mathcal{Q}_2 and the Higgs branch of $\mathcal{Q}_{4.11}$ are the same.

It is straightforward to compute the Higgs branch Hilbert series of $\mathcal{Q}_{4.11}$ to find agreement

$$\mathcal{H}(\mathcal{Q}_{4.11}) = \mathcal{C}(\mathcal{Q}_2) \quad (4.12)$$

In particular this makes \mathcal{Q}_2 an example of a magnetic quiver for a rank-3 four dimensional theory. Magnetic quivers for rank-1 and rank-2 theories were studied in [13, 15]. The $\text{O}(1) \simeq \mathbb{Z}_2$ flavour symmetry in $\mathcal{Q}_{4.11}$ is expressed in \mathcal{Q}_2 as the \mathbb{Z}_2 exchanging the two $\text{U}(3)$ gauge nodes.

4.2 $(\overline{\text{min.}E_6} \times \mathbb{H}^{12}) // \text{Sp}(2)$

There is another proposed duality in [19, Table 2 Ex. 16] which states that the $\text{Sp}(2)$ flavour symmetry gauging of the rank 1 E_6 SCFT [34–37] coupled to 12 free hyps is dual to $\text{SU}(4)$ with four fundamental flavours and two anti-symmetric.

The electric quiver is given below

$$\begin{array}{c}
 \square \\
 | \\
 \bullet \xrightarrow{\wedge^2} \blacksquare \\
 \text{SU}(4) \quad \text{Sp}(2)
 \end{array}
 \tag{4.13}$$

with the (unrefined) Higgs branch Hilbert series computed as

$$\text{HS}[\mathcal{H}(\mathcal{Q}_{4.13})] = \frac{\left(\begin{array}{l} 1 + 17t^2 + 36t^3 + 220t^4 + 564t^5 + 2192t^6 + 5456t^7 + 15897t^8 + 35388t^9 + 84385t^{10} \\ + 165040t^{11} + 330357t^{12} + 558676t^{13} + 948191t^{14} + 1360392t^{15} + 1931582t^{16} \\ + 2222620t^{17} + 2460927t^{18} + 1755844t^{19} + 745362t^{20} - 1855388t^{21} - 4328851t^{22} \\ - 8203044t^{23} - 10166289t^{24} - 12396256t^{25} - 10389664t^{26} - 8125224t^{27} - 936407t^{28} \\ + 4603732t^{29} + 13037971t^{30} + 16246308t^{31} + 19779930t^{32} + \dots + t^{64} \end{array} \right)}{(1-t^2)^9(1-t^3)^{12}(1-t^4)^9}
 \tag{4.14}$$

The Hilbert series shows that the moduli space has global symmetry $U(4) \times \text{Sp}(2)$ as expected. The (quaternionic) dimension of the Higgs branch is 13 from counting $\dim \mathcal{H}(\mathcal{Q}_{4.13}) = \#\text{hypers} - \#\text{vectors}$. This is not immediately apparent in the Hilbert series above due to negative terms in the numerator, however the order of the pole of the Hilbert series at $t = 1$ is indeed 26 which means that the quaternionic dimension is 13.

The proposed dual to $\mathcal{Q}_{4.13}$ takes the rank 1 E_6 theory coupled to 12 free hypers and gauges $\text{Sp}(2)$. In terms of magnetic quivers, the rank 1 E_6 theory has a magnetic quiver given by the affine $E_6^{(1)}$ quiver. The coupling of twelve free hypers can be done by the method of *quiver extension* [5] which is a form of quiver addition. The quiver extension needed in this example adds the finite A_4 quiver three times to the $E_6^{(1)}$ quiver resulting in the following magnetic quiver for the rank 1 E_6 theory coupled to 12 free hypers

$$\begin{array}{cccccccc}
 & & & & & \circ 1 & & \\
 & & & & & | & & \\
 & & & & & \circ 2 & & \\
 & & & & & | & & \\
 \circ & - & \circ \\
 1 & & 2 & & 3 & & 4 & & 4 & & 4 & & 2 & & 1
 \end{array}
 \tag{4.15}$$

The $\text{Sp}(2)$ gauging proceeds with quotient quiver subtraction shown in Figure 4 to produce \mathcal{Q}_4 . Computation of the Coulomb branch Hilbert series indeed confirms that

$$\mathcal{C}(\mathcal{Q}_4) = \mathcal{H}(\mathcal{Q}_{4.13})
 \tag{4.16}$$

so \mathcal{Q}_4 is a magnetic quiver for the Higgs branch of the $4d \mathcal{N} = 2$ theory $\mathcal{Q}_{4.13}$. The Coulomb and Higgs branch Hasse diagrams are shown in Figure 5.

This magnetic quiver was proposed in [39] through methods studying the theory $\mathcal{Q}_{4.13}$ as a class \mathcal{S} theory and considering its S-dual frames. It may also be found from the explicit Type IIA brane system for $\text{SU}(4)$ gauge theory with four flavours and two anti-symmetric [21]. Quotient quiver subtraction provides an alternative construction for the magnetic quiver.

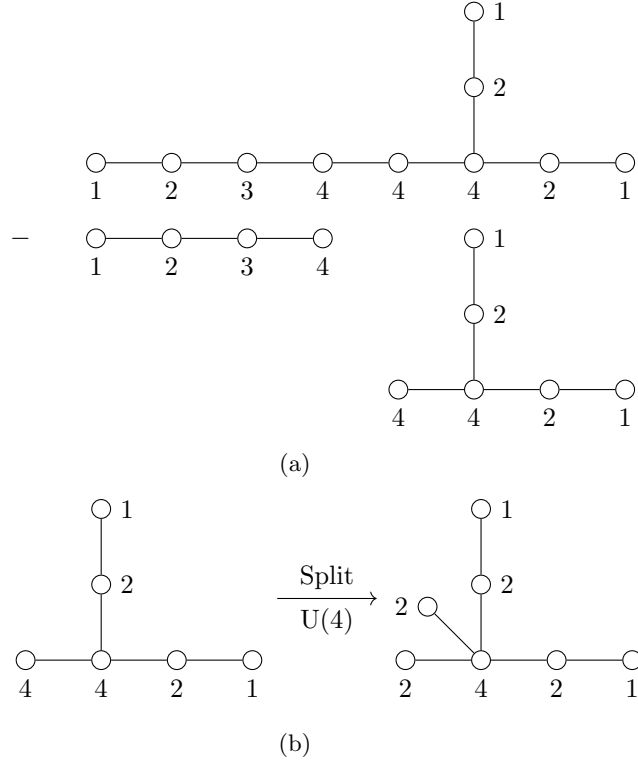


Figure 4: $\text{Sp}(2)$ quotient quiver subtraction on the extended affine $E_6^{(1)}$ quiver $\mathcal{Q}_{4.15}$ which occurs in two steps. The first step is shown in 4a and involves the subtraction of the $\text{Sp}(2)$ quotient quiver from the maximal leg. The second step, shown 4b, is the splitting of the $\text{U}(4)$ node into two $\text{U}(2)$ nodes producing the resulting quiver \mathcal{Q}_4 .

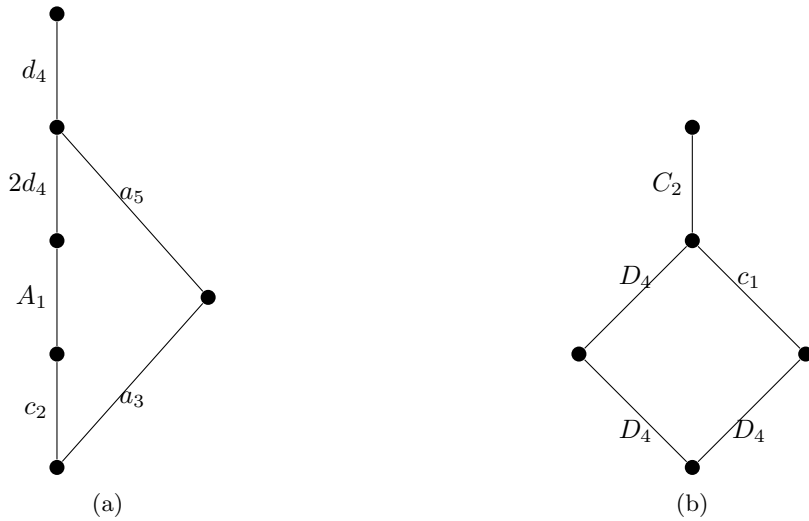


Figure 5: Hasse diagrams for the Coulomb and Higgs branches of \mathcal{Q}_4 shown in Figure 5a and Figure 5b respectively.

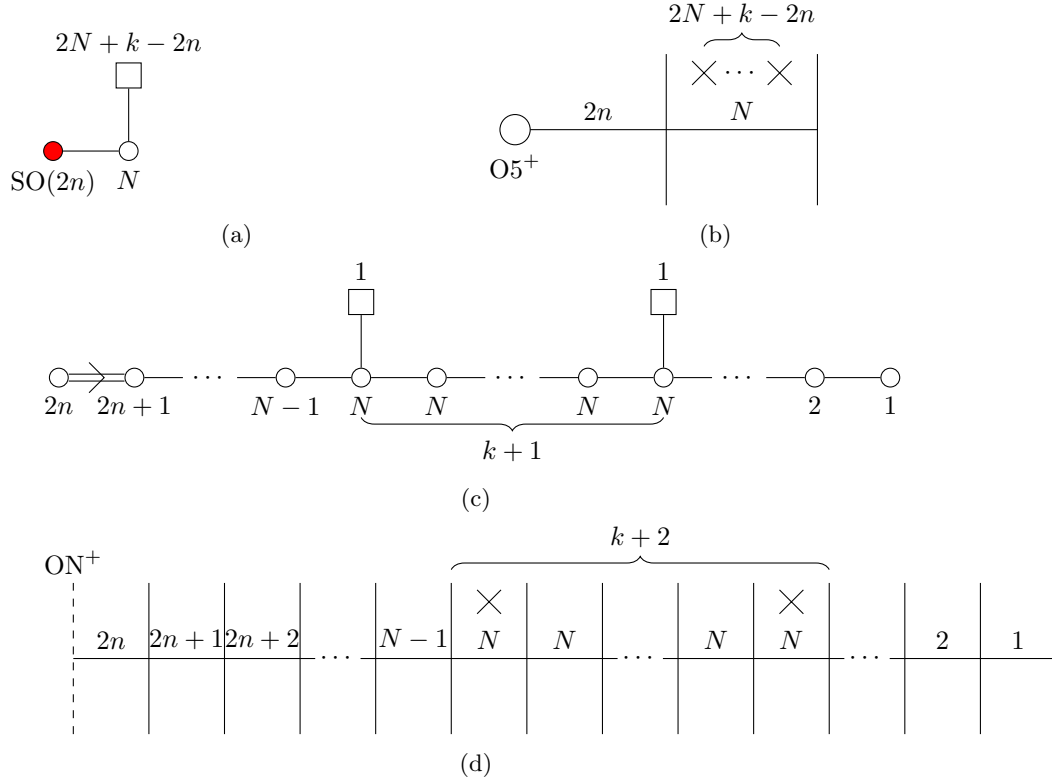


Figure 7: Gauging an $SO(2n)$ flavour subgroup of $U(N)$ SQCD with $2N+k$ flavours returns the theory in Figure 7a, realised from the brane system in Figure 7b. The magnetic theory is conjectured to be Figure 7c, associated to the brane system in Figure 7d, related to that of Figure 7b by brane-creation and S-duality. Comparison to the mirror of the SQCD in (4.1) leads to the conjectural quotient quiver (5.1).

1. Take a target quiver with a long leg of gauge nodes up to at least $U(2n)$. As in Section 4, the edge in teal denotes some generic connection to the rest of the quiver Q .

$$\begin{array}{c}
 \circ \text{---} \circ \text{---} \dots \text{---} \circ \text{---} \circ \text{---} \textcircled{Q} \\
 1 \quad 2 \quad \quad \quad 2n-1 \quad 2n
 \end{array} \tag{5.2}$$

2. Align the $SO(2n)$ quotient quiver (5.1) against the leg of the target quiver and subtract the ranks of the quotient quiver from those of the target. This deletes the gauge nodes from $U(1)$ up to $U(2n-1)$ in the maximal chain, leaving only $U(2n)$. Rebalancing is not required.

$$\begin{array}{c}
 \circ \text{---} \circ \text{---} \dots \text{---} \circ \text{---} \circ \text{---} \textcircled{Q} \\
 1 \quad 2 \quad \quad \quad 2n-1 \quad 2n \\
 - \\
 \circ \text{---} \circ \text{---} \dots \text{---} \circ \\
 1 \quad 2 \quad \quad \quad 2n-1 \\
 \\
 \circ \text{---} \textcircled{Q} \\
 2n
 \end{array} \tag{5.3}$$

3. All edges connected to the $U(2n)$ gauge node double their non-simply laced-ness – the $U(2n)$ is the long root.

$$\begin{array}{ccc}
 \text{○} & \xrightarrow{\text{Lacing}} & \text{○} \Rightarrow \text{○} \\
 2n & & 2n \quad Q
 \end{array} \tag{5.4}$$

Note that $SO(2n)$ quotient quiver subtraction requires a leg of gauge nodes $(1) - (2) - \dots - (2n) -$, sourcing (at least) an $SU(2n)$ factor in the Coulomb branch global symmetry. The $SO(2n)$ being gauged is embedded in this $SU(2n)$ with discrete commutant, shown below.

$$[1, 0, \dots, 0, 1]_{SU(2n)} \rightarrow [0, 1, 0, \dots, 0]_{SO(2n)} + [2, 0, \dots, 0]_{SO(2n)} \tag{5.5}$$

In the case that the target quiver has enhanced global symmetry, the $SO(2n)$ being gauged may be embedded directly into that global symmetry. Nevertheless, it remains sourced by the long leg.

5.1 $\overline{min.F_4} // SO(2)$

The affine $F_4^{(1)}$ quiver has Coulomb branch $\overline{min.F_4}$. It contains a tail of gauge nodes on the long side of the quiver which goes as $(1) - (2) - (3) -$ and is suitable for $SO(2)$ quotient quiver subtraction. This operation is shown in Figure 8 and produces \mathcal{Q}_8 , with the subtraction of the quotient quiver in Figure 8a and the non-simple lacing in Figure 8b.

The refined Coulomb branch Hilbert series of Figure 8 is cumbersome. However, the unrefined Coulomb branch Hilbert series is

$$\text{HS}[\mathcal{C}(\mathcal{Q}_8)] = \frac{\left(1 + 14t^2 + 168t^4 + 854t^6 + 3136t^8 + 7062t^{10} + 11991t^{12} + 13708t^{14} + 11991t^{16} + 7062t^{18} + 3136t^{20} + 854t^{22} + 168t^{24} + 14t^{26} + t^{28} \right)}{(1-t^2)^7(1-t^4)^7} \tag{5.6}$$

Although this moduli space has no particular name, its $Sp(3)$ symmetry can be confirmed from the refined Hilbert series (not presented here). The Coulomb branch Hasse diagram is also straightforwardly computed and given in Figure 8c. It is still unclear how to compute the Higgs branch Hasse diagram for non-simply laced quivers [32].

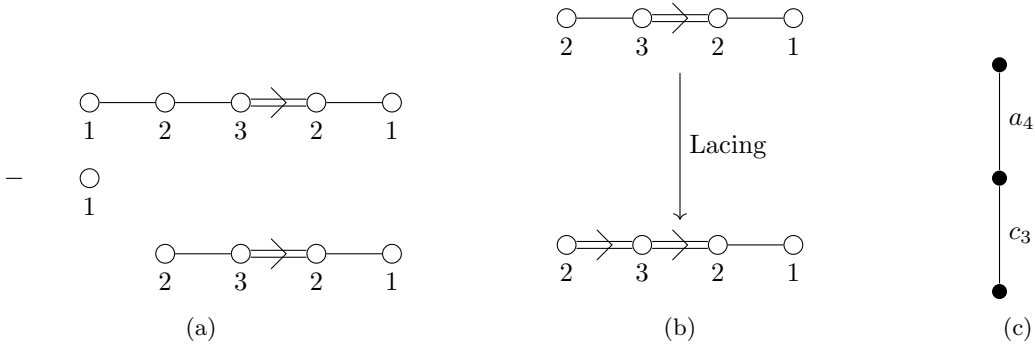


Figure 8: $SO(2)$ quotient quiver subtraction on the affine $F_4^{(1)}$ quiver occurs in two steps. The first is shown in 8a and involves the subtraction of the $SO(2)$ quotient quiver from the maximal leg. The second step, given in 8b, is the non-simple lacing of the edge connecting the left $U(2)$ node to the $U(3)$, producing the resulting quiver \mathcal{Q}_8 . The Coulomb branch Hasse diagram is given in Figure 8c.

The conclusion is that

$$\overline{\min.F_4} // \text{SO}(2) = \mathcal{C}(\mathcal{Q}_8) \quad (5.7)$$

which is further verified from an explicit Weyl integration.

The following embedding of $F_4 \hookrightarrow \text{Sp}(3) \times \text{U}(1)$ is employed where the fundamental representation of F_4 decomposes as

$$(\mu_1)_{F_4} \rightarrow \mu_1(q + 1/q) + \mu_2 \quad (5.8)$$

where the $\mu_{1,2}$ on the right hand side refer to $\text{Sp}(3)$ highest weight fugacities and q is a $\text{U}(1)$ fugacity.

5.2 $\overline{\min.E_7} // \text{SO}(4)$

The affine $E_7^{(1)}$ quiver has Coulomb branch $\overline{\min.E_7}$. Its two maximal legs of (1) – (2) – (3) – (4) – each support an $\text{SO}(4)$ quotient quiver subtraction. One such subtraction, shown explicitly in Figure 9, produces \mathcal{Q}_9 . Although its refined Coulomb branch Hilbert series is cumbersome, the unrefined expression is

$$\text{HS}[\mathcal{C}(\mathcal{Q}_9)] = \frac{\left(1 + 7t^2 + 100t^4 + 596t^6 + 3531t^8 + 13712t^{10} + 45536t^{12} + 112650t^{14} + 233881t^{16} + 380039t^{18} + 519199t^{20} + 565768t^{22} + \dots + t^{44}\right)}{(1-t^2)^{11}(1-t^4)^{11}} \quad (5.9)$$

This moduli space, which has no particular name, has $\text{SO}(6) \times \text{SU}(2)$ symmetry, confirmed by the refined Hilbert series.

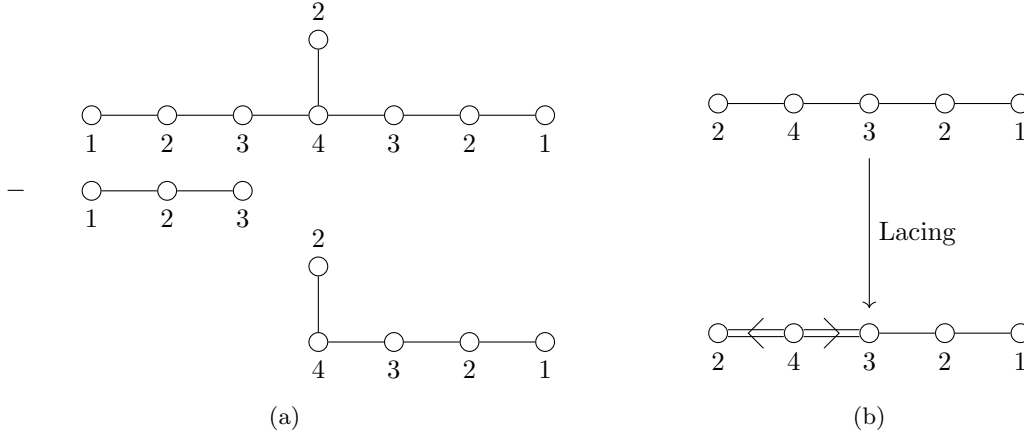


Figure 9: $\text{SO}(4)$ quotient quiver subtraction on the affine $E_7^{(1)}$ quiver occurs in two steps. The first step, shown in 9a, involves the subtraction of the $\text{SO}(4)$ quotient quiver from one maximal leg. The second step, in 9b, is the non-simple lacing of the two edges emerging from the $\text{U}(4)$ node.

The same moduli space arises from Weyl integration and the embedding $E_7 \hookrightarrow D_6 \times A_1 \hookrightarrow D_3 \times D_3 \times A_1 \hookrightarrow D_2 \times D_3 \times A_1$ which decomposes the $[0, 0, 0, 0, 1, 0]$ of E_7 as

$$(\mu_6)_{E_7} \rightarrow (\mu_1 + \nu_1^2 + \nu_2^2) \rho + (\mu_2 + \mu_3) \nu_1 \nu_2 \quad (5.10)$$

Note that the μ, ν , and ρ are highest weight fugacities for D_3 , D_2 , and A_1 respectively. The integration is performed with respect to the D_2 fugacities.

5.3 $\overline{\min.E_8}/\text{SO}(4)$

Consider again the affine $E_8^{(1)}$ quiver, whose maximal leg $(1) - (2) - \dots - (6) -$ admits an $\text{SO}(4)$ quotient quiver subtraction. This operation, shown in Figure 10, produces \mathcal{Q}_{10} .

The refined Coulomb branch Hilbert series of Figure 10 is cumbersome – its unrefined form is

$$\text{HS}[\mathcal{C}(\mathcal{Q}_{10})] = \frac{\left(\begin{aligned} &1 + 22t^2 + 582t^4 + 10360t^6 + 154981t^8 + 1822118t^{10} + 17548922t^{12} + 139175916t^{14} \\ &+ 925774625t^{16} + 5219073951t^{18} + 25226111030t^{20} + 105435301585t^{22} \\ &+ 384139161711t^{24} + 1227840826079t^{26} + 3462893979058t^{28} + 8658011097494t^{30} \\ &+ 19269044472299t^{32} + 38301892953919t^{34} + 68192783223365t^{36} \\ &+ 108993744295329t^{38} + 156680149569483t^{40} + 202847214133311t^{42} \\ &+ 236754481344743t^{44} + 249255260007352t^{46} + \dots + t^{92} \end{aligned} \right)}{(1-t^2)^{23}(1-t^4)^{23}} \quad (5.11)$$

This moduli space, which has no particular name as a symplectic singularity, has $\text{SO}(10)$ global symmetry.

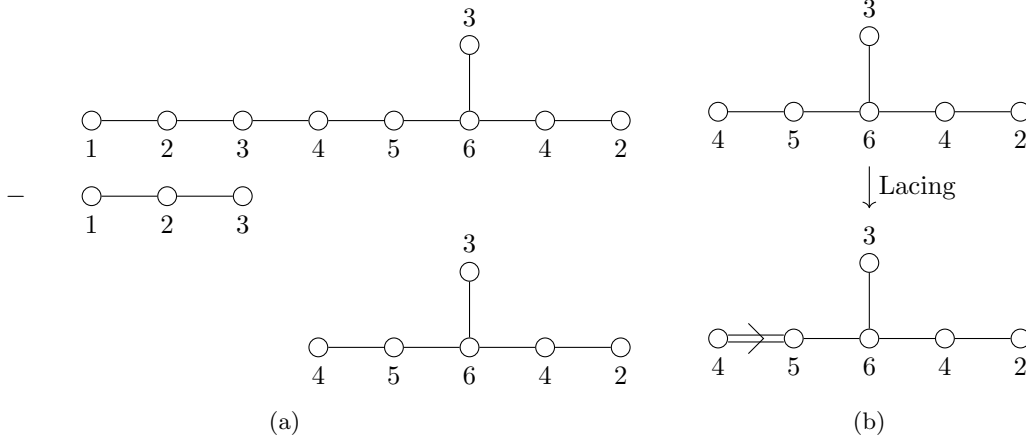


Figure 10: $\text{SO}(4)$ quotient quiver subtraction on the affine $E_8^{(1)}$ quiver occurs in two steps. The first step is shown in 10a and involves the subtraction of the $\text{SO}(4)$ quotient quiver from the maximal leg. The second step, shown 10b, is the non-simple lacing of the two edges going from the $\text{U}(4)$ node producing \mathcal{Q}_{10} .

Weyl integration straightforwardly constructs the same moduli space under the embedding $E_8 \hookrightarrow D_8 \hookrightarrow \times A_3 \hookrightarrow D_5 \hookrightarrow D_2 \times D_5$, which decomposes the adjoint of E_8 as

$$(\mu_7)_{E_8} \rightarrow \mu_2 + (1 + \mu_1)\nu_1^2 + (\mu_4 + \mu_5)\nu_1\nu_2 + (1 + \mu_1)\nu_2^2 + \nu_1^2\nu_2^2 \quad (5.12)$$

The μ and ν are highest weight fugacities for D_5 and D_2 respectively and the integration is performed with respect to the D_2 fugacities.

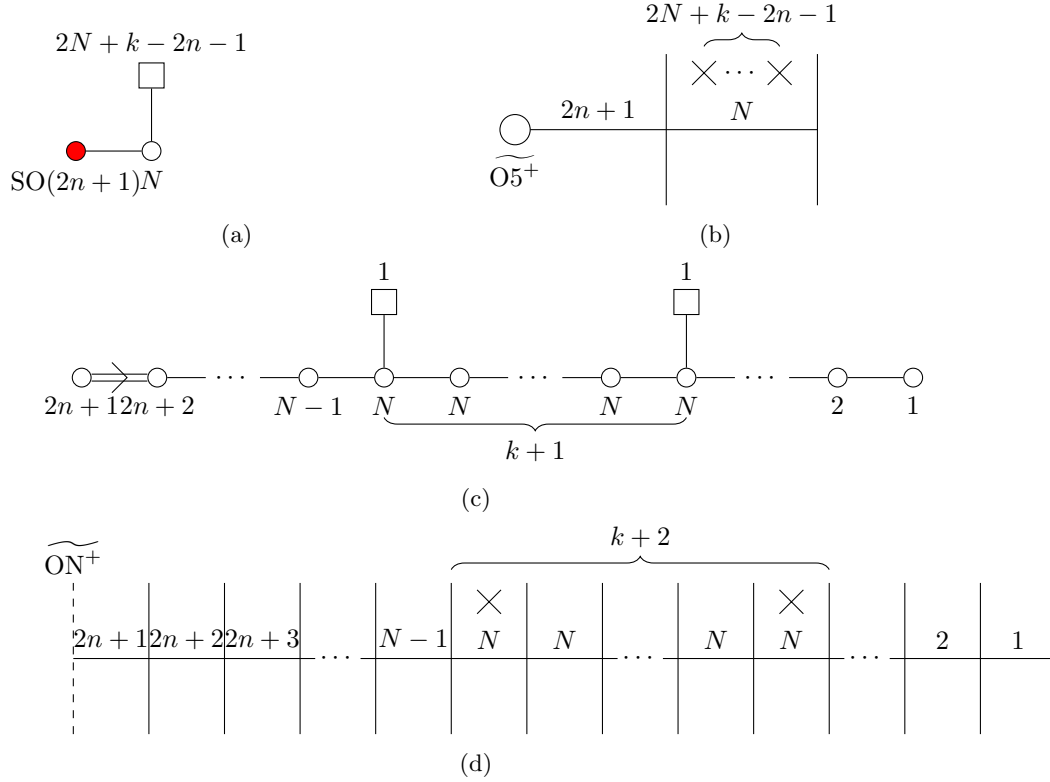


Figure 11: Gauging an $\text{SO}(2n+1)$ flavour subgroup of $\text{U}(N)$ SQCD with $2N+k$ flavours returns the theory in Figure 11a, realised from the brane system in Figure 11b. The magnetic theory is conjectured to be Figure 11c, associated to the brane system in Figure 11d, related to that of Figure 11b by brane-creation and S-duality. Comparison to the mirror of the SQCD in (4.1) leads to the conjectural quotient quiver (6.1).

6 $\text{SO}(2n+1)$ Quotient Quivers

The starting point for the analysis is once again the $\text{U}(N)$ SQCD with $2N+k$ flavours given in (4.1). Gauging an $\text{SO}(2n+1)$ flavour symmetry subgroup results in the theory \mathcal{Q}_{11a} given in Figure 11a with Type IIB brane system in Figure 11b. The magnetic theory is \mathcal{Q}_{11c} given in Figure 11c, alongside its brane system in Figure 11d. Comparing the magnetic theory of the SQCD before ((4.1)) and after (Figure 11c) gauging identifies the quotient quiver (6.1) and the subtraction prescription, given below. The total rank of gauge nodes in the quotient quiver is $n(2n+1) = \dim(\text{SO}(2n+1))$.

$$\text{SO}(2n+1) \text{ Quotient Quiver} \quad \begin{array}{cccc} \circ & \circ & \cdots & \circ & \circ \\ 1 & 2 & & 2n-1 & 2n \end{array} \quad (6.1)$$

The gauging algorithm, which is almost identical to the $\text{SO}(2n)$ case, is given below for completeness.

Formal Statement of the Rule

1. Take a target quiver with a long leg of gauge nodes up to at least $\text{U}(2n+1)$. The edge in teal denotes some generic connection to the rest of the quiver \mathcal{Q} – the only restriction is that the

long leg must correspond to long roots of the Coulomb branch global symmetry algebra.

$$\begin{array}{c}
 \textcircled{1} \text{---} \textcircled{2} \text{---} \cdots \text{---} \textcircled{2n} \text{---} \textcircled{2n+1} \text{---} \textcircled{Q} \\
 1 \quad 2 \quad \quad \quad 2n \quad 2n+1 \\
 \textcircled{1} \text{---} \textcircled{2} \text{---} \cdots \text{---} \textcircled{2n} \\
 1 \quad 2 \quad \quad \quad 2n
 \end{array} \tag{6.2}$$

- Align end of the $\text{SO}(2n+1)$ quotient quiver against the leg of the target quiver and subtract the ranks of the quotient quiver from those of the target. This deletes the gauge nodes from $\text{U}(1)$ up to $\text{U}(2n)$ in the maximal chain, leaving only $\text{U}(2n+1)$. Rebalancing is not required.

$$\begin{array}{c}
 \textcircled{1} \text{---} \textcircled{2} \text{---} \cdots \text{---} \textcircled{2n} \text{---} \textcircled{2n+1} \text{---} \textcircled{Q} \\
 1 \quad 2 \quad \quad \quad 2n \quad 2n+1 \\
 - \\
 \textcircled{1} \text{---} \textcircled{2} \text{---} \cdots \text{---} \textcircled{2n} \\
 1 \quad 2 \quad \quad \quad 2n \\
 \\
 \textcircled{2n+1} \text{---} \textcircled{Q} \\
 2n+1
 \end{array} \tag{6.3}$$

- All edges connected to the $\text{U}(2n+1)$ gauge node (shown in teal) double their non-simply lacedness, with the $\text{U}(2n+1)$ corresponding to the long root.

$$\textcircled{2n+1} \text{---} \textcircled{Q} \xrightarrow{\text{Lacing}} \textcircled{2n+1} \rightleftarrows \textcircled{Q} \tag{6.4}$$

Note that $\text{SO}(2n+1)$ quotient quiver subtraction requires a $(1) - (2) - \cdots - (2n+1)$ - long leg of gauge nodes, which sources (at least) an $\text{SU}(2n+1)$ factor of the Coulomb branch global symmetry. The $\text{SO}(2n+1)$ to be gauged is embedded with discrete commutant as follows.

$$[1, 0, \cdots, 0, 1]_{\text{SU}(2n+1)} \rightarrow [0, 1, 0, \cdots, 0]_{\text{SO}(2n+1)} + [2, 0, \cdots, 0]_{\text{SO}(2n+1)} \tag{6.5}$$

This is exactly analogous to the embedding used for $\text{SO}(2n)$ quotient quiver subtraction. If the target quiver has enhanced global symmetry, the $\text{SO}(2n+1)$ being gauged may be embedded directly into that global symmetry. The origin remains in the gauge nodes in the long leg.

It is important to address the various degeneracies inspired by accidental isomorphisms. The $A_1 \cong B_1 \cong C_1$ isomorphism is particularly interesting as it establishes that $\text{SU}(2)$ and $\text{Sp}(1)$ quotient quiver subtraction are identical operations. Interestingly, $\text{SO}(3)$ quotient quiver subtraction differs, and the B_1 embedding in the global symmetry of the long leg is distinct to that for A_1 and C_1 . Explicitly, $\text{SO}(3)$ is embedded inside an $\text{SU}(3)$ of the long leg whereas $\text{SU}(2)$ and $\text{Sp}(1)$ are embedded inside $\text{SU}(2)$. For similar reasons the $B_2 \cong C_2$ isomorphism does not extend to $\text{SO}(5)$ and $\text{Sp}(2)$ quotient quiver subtraction, both because the resulting quivers are different and because $\text{SO}(5)$ is embedded inside $\text{SU}(5)$ and $\text{Sp}(2)$ is embedded inside $\text{SU}(4)$.

6.1 $\overline{\min.E_6}/\!/SO(3)$

The affine $E_6^{(1)}$ quiver's (1) – (2) – (3)– long leg is amenable to $SO(3)$ quotient quiver subtraction. This is shown in Figure 12 and returns \mathcal{Q}_{12} . The refined Coulomb branch Hilbert series is unwieldy – the unrefined Coulomb branch Hilbert series is

$$\text{HS}[\mathcal{C}(\mathcal{Q}_{12})] = \frac{\left(1 + 8t^2 + 99t^4 + 479t^6 + 2095t^8 + 5355t^{10} + 11577t^{12} + 16622t^{14} + 20072t^{16} + 16622t^{18} + 11577t^{20} + 5355t^{22} + 2095t^{24} + 479t^{26} + 99t^{28} + 8t^{30} + t^{32}\right)}{(1-t^2)^8(1-t^4)^8} \quad (6.6)$$

This moduli space, which has no particular name as a symplectic singularity, has $SU(3) \times SU(3)$ symmetry, confirmed at the level of the refined Hilbert series. The same moduli space may be found

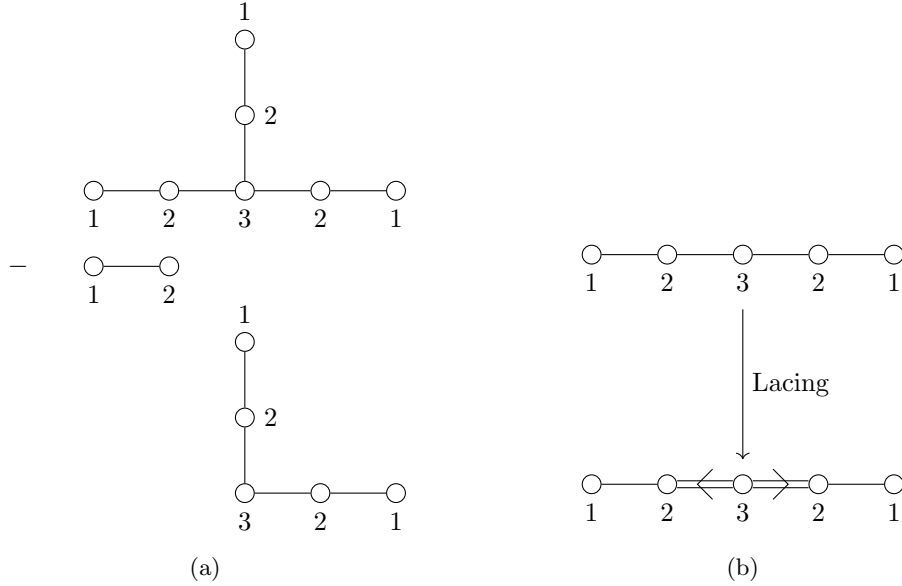


Figure 12: $SO(3)$ quotient quiver subtraction on the affine $E_6^{(1)}$ quiver which occurs in two steps. The first step is shown in Figure 12a and involves the subtraction of the $SO(3)$ quotient quiver from one maximal leg. The second step, shown in Figure 12b, is the non-simple lacing of the two edges going from the $U(3)$ node producing \mathcal{Q}_{12} .

through an explicit computation with Weyl integration. This requires the following embedding of $E_6 \leftrightarrow A_2 \times A_2 \times A_2 \leftrightarrow A_2 \times A_2 \times A_1$ which decomposes the $[1, 0, 0, 0, 0, 0]$ of E_6 as

$$(\mu_1)_{E_6} \rightarrow \mu_2 \nu_2 + (\mu_1 + \nu_1) \rho^2 \quad (6.7)$$

where the μ, ν , and ρ are highest weight fugacities for A_2, A_2 , and A_1 respectively. The integration is performed with respect to the A_1 fugacity.

This is the second hyper-Kähler quotient construction of the Coulomb branch of \mathcal{Q}_{12} using exceptional nilpotent orbits. The first used $SU(3)$ chain polymerisation of two affine $F_4^{(1)}$ quivers [2, 5] and yields the following equalities

$$\overline{\min.E_6}/\!/SO(3) = (\overline{\min.F_4} \times \overline{\min.F_4})/\!/SU(3) = \mathcal{C}[\mathcal{Q}_{12}] \quad (6.8)$$

6.2 $\overline{\min.F_4}/\text{SO}(3)$

The affine $F_4^{(1)}$ quiver's (1) – (2) – (3)– long leg is also amenable to an $\text{SO}(3)$ quotient quiver subtraction. This operation is shown in Figure 13 and produces \mathcal{Q}_{13} , with the subtraction of the quotient quiver in Figure 13a and the non-simple lacing in Figure 13b. It is important in the non-simple lacing step to note that the edge connecting the $\text{U}(3)$ and $\text{U}(2)$ goes from multiplicity two to multiplicity four.

The refined Coulomb branch Hilbert series of Figure 13 is cumbersome to present, however the unrefined Coulomb branch Hilbert series is presented as

$$\text{HS}[\mathcal{C}(\mathcal{Q}_{13})] = \frac{1 + 3t^2 + 31t^4 + 55t^6 + 156t^8 + 132t^{10} + 156t^{12} + 55t^{14} + 31t^{16} + 3t^{18} + t^{20}}{(1-t^2)^5(1-t^4)^5} \quad (6.9)$$

This moduli space has no particular name as a symplectic singularity but it does have $\text{SU}(3)$ symmetry which can be confirmed from the refined Hilbert series (not presented here). Further support for this global symmetry takes of the form of the Coulomb branch Hasse diagram drawn in Figure 13c. The

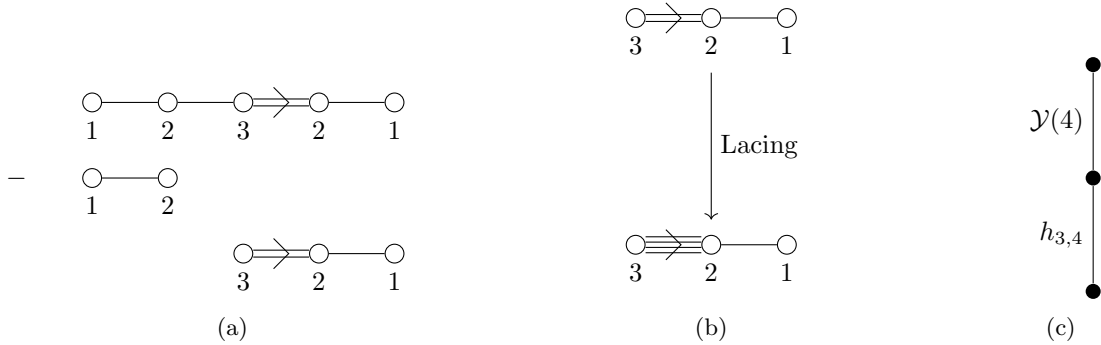


Figure 13: $\text{SO}(3)$ quotient quiver subtraction on the affine $F_4^{(1)}$ quiver occurs in two steps. The first step is shown in Figure 13a and involves the subtraction of the $\text{SO}(3)$ quotient quiver from one maximal leg. The second step, shown in Figure 13b, is the non-simple lacing of the two edges going from the $\text{U}(3)$ node producing \mathcal{Q}_{13} . Note that the non-simply laced-ness of this edge goes from two to four. The Coulomb branch Hasse diagram is given in Figure 13c.

same moduli space emerges from Weyl integration with the embedding $F_4 \leftrightarrow A_2 \times A_2 \leftrightarrow A_2 \times A_1$ decomposing the $[1, 0, 0, 0]$ of F_4 as

$$(\mu_1)_{F_4} \rightarrow \mu_1\mu_2 + (1 + \mu_1^2 + \mu_2^2)\nu^2 + \nu^4 \quad (6.10)$$

Note that μ and ν are highest weight fugacities for A_2 and A_1 respectively. The integration is performed with respect to the A_1 fugacity.

This quiver \mathcal{Q}_{13} may be thought of as the folding [40] of \mathcal{Q}_{12} . This is an example of the commutation of quotient quiver subtraction and discrete operations on quivers, first noted in [1].

The quiver \mathcal{Q}_{13} is also believed to be a magnetic quiver for the $4d \mathcal{N} = 2$ rank-1 theory with flavour symmetry A_2 . This theory has been conjectured to be derived from the T^2 compactification with \mathbb{Z}_4 twist of the $6d \mathcal{N} = (1, 0)$ $\text{SU}(4)$ gauge theory with 12 flavours and an anti-symmetric [41]. The $\text{SO}(3)$ quotient quiver subtraction in Figure 13 is suggestive of another construction of the Higgs

branch of the rank-1 A_2 theory

$$\mathcal{H}(T_3^{\mathbb{Z}_2})//\text{SO}(3) = \overline{\text{min.F}_4} // \text{SO}(3) = \mathcal{H}(A_2) \quad (6.11)$$

where the T^3 theory enjoys a \mathbb{Z}_2 twist which changes the Higgs branch from $\overline{\text{min.E}_6}$ to $\overline{\text{min.F}_4}$ [42], seen in the magnetic quiver through folding [40].

7 $\text{Sp}(n) + \frac{1}{2}\text{F}$ Quotient Quivers

In Sections 4, 5, and 6 a quotient quiver subtraction algorithm was presented to gauge $\text{Sp}(n)$ and $\text{SO}(n)$ subgroups of Coulomb branch global symmetries. Key to these derivations were Type IIB brane systems in the electric phase in the presence of $\text{O}5^\mp$ and $\text{O}5^+$.

The final orientifold to complete the quartet is the $\widetilde{\text{O}5^-}$. The starting point for the analysis is the $\text{U}(N)$ SQCD with $2N + k$ flavours where k is positive, this parameterisation is for convenience but will not play a role in the resulting quotient quiver subtraction algorithm. Now consider coupling a half-hypermultiplet of $\text{Sp}(n)$ and gauge the $\text{Sp}(n)$ resulting in

$$\begin{array}{ccc}
 & 2N + k - 2n & \\
 & \square & \blacksquare \text{ O}(1) \\
 & | & | \\
 & \circ & \bullet \\
 N & \text{Sp}(n) &
 \end{array} \quad (7.1)$$

Immediately it is clear that this theory suffers from a Witten anomaly [38] due to the half-hypermultiplet coupled to $\text{Sp}(n)$. As an academic exercise, one may consider the effect of this operation of gauging $\text{Sp}(n)$ with a half-hyper on the magnetic quiver with the aim of this gauging to construct moduli spaces.

Comparing the magnetic theory of the SQCD before (4.1) and after gauging (Figure 14c) identifies the quotient quiver (7.2) and the subtraction prescription. The $\text{Sp}(n) + \frac{1}{2}\text{F}$ quotient quiver is

$$\begin{array}{ccccccc}
 & & & & 2n - 2 & & \\
 \circ & \text{---} & \circ & \text{---} & \cdots & \text{---} & \circ & \text{---} & \circ \\
 1 & & 2 & & & & 2n - 1 & &
 \end{array} \quad (7.2)$$

which has total gauge node rank of $n(2n - 1)$, which is n short of the expected dimension reduction of gauging $\text{Sp}(n)$ and adding a half-hyper, $2n^2$. However one should note that the leftmost gauge node in the quiver shown in Figure 14c is $\text{U}(n)$ rather than $\text{U}(2n)$, this reduction of the rank by n compensates for the total rank of gauge nodes in the quotient quiver.

Formal Statement of the Rule

1. Take a target quiver with a long leg of gauge nodes up to at least $\text{U}(2n)$. The edge in teal denotes some generic connection to the rest of the quiver \mathcal{Q} – the only restriction is that the long leg must correspond to long roots of the Coulomb branch global symmetry algebra.

$$\begin{array}{ccccccc}
 \circ & \text{---} & \circ & \text{---} & \cdots & \text{---} & \circ & \text{---} & \circ & \text{---} & \circ \\
 1 & & 2 & & & & 2n - 1 & & 2n & & \mathcal{Q}
 \end{array} \quad (7.3)$$

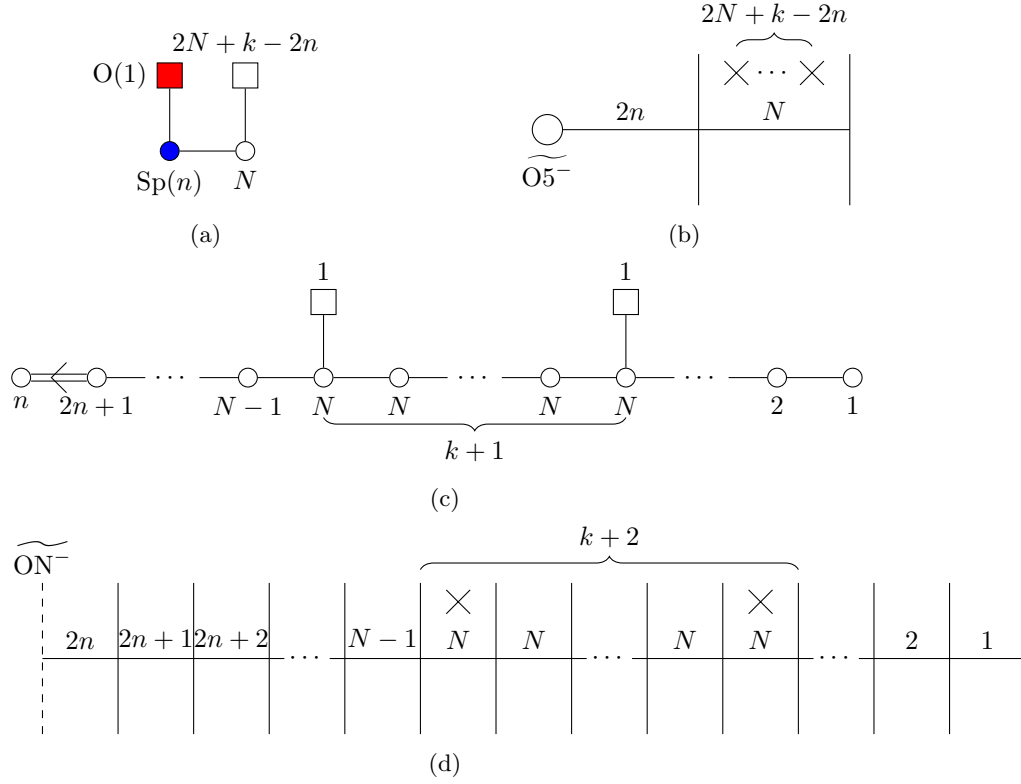


Figure 14: Gauging an $\mathrm{Sp}(n) + \frac{1}{2}\mathrm{F}$ flavour subgroup of $\mathrm{U}(N)$ SQCD with $2N + k$ flavours returns the theory in Figure 14a, realised from the brane system in Figure 14b. The magnetic theory is conjectured to be Figure 14c, associated to the brane system in Figure 14d, related to that of Figure 14b by brane-creation and S-duality. Comparison to the mirror of the SQCD in (4.1) leads to the conjectural quotient quiver (7.2).

- Align end of the $\mathrm{Sp}(n) + \frac{1}{2}\mathrm{F}$ quotient quiver against the leg of the target quiver and subtract the ranks of the quotient quiver from those of the target. This deletes the gauge nodes from $\mathrm{U}(1)$ up to $\mathrm{U}(2n - 1)$ in the maximal chain, leaving only $\mathrm{U}(2n)$. Rebalancing is not required.

$$\begin{array}{c}
 \begin{array}{ccccccc}
 \circ & \circ & \cdots & \circ & \circ & \circ & \circ \\
 1 & 2 & & 2n-1 & 2n & & Q \\
 \hline
 \circ & \circ & \cdots & \circ & & & \\
 1 & 2 & & 2n-1 & & & \\
 \hline
 & & & & \circ & \circ & \\
 & & & & 2n & & Q
 \end{array} \\
 - \\
 \begin{array}{c}
 \circ & \circ & \cdots & \circ & \circ & \circ & \circ \\
 1 & 2 & & 2n-1 & & & \\
 \hline
 & & & & \circ & \circ & \\
 & & & & 2n & & Q
 \end{array} \\
 \hline
 \begin{array}{c}
 \circ & \circ & \cdots & \circ & \circ & \circ & \circ \\
 1 & 2 & & 2n-1 & & & \\
 \hline
 & & & & \circ & \circ & \\
 & & & & 2n & & Q
 \end{array}
 \end{array} \tag{7.4}$$

- The resulting $\mathrm{U}(2n)$ gauge node has its rank halved to become $\mathrm{U}(n)$ and all edges in teal double

their non-simply lacedness with the $U(n)$ node being short.

$$\begin{array}{c}
 \circ \text{---} \textcircled{Q} \\
 2n
 \end{array}
 \xrightarrow{\text{Halve rank}}
 \begin{array}{c}
 \circ \text{---} \textcircled{Q} \\
 n
 \end{array}
 \xrightarrow{\text{Double lacing}}
 \begin{array}{c}
 \circ \text{---} \textcircled{Q} \\
 n
 \end{array}
 \quad (7.5)$$

7.1 $(\overline{\text{min.}E_6} \times \mathbb{H}) // \text{Sp}(1)$

A simple but non-trivial example of the $\text{Sp}(1) + \frac{1}{2}\text{F}$ quotient quiver subtraction is performed on the affine $E_6^{(1)}$ quiver to produce \mathcal{Q}_{15} as shown in Figure 15.

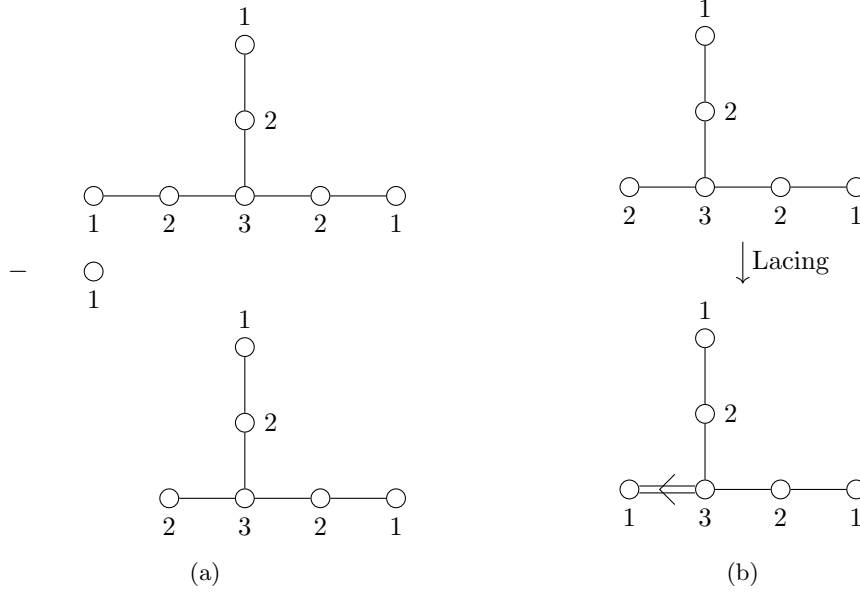


Figure 15: $\text{Sp}(1) + \frac{1}{2}\text{F}$ quotient quiver subtraction on the affine $E_6^{(1)}$ quiver which occurs in two steps. The first step is shown in Figure 15a and involves the subtraction of the $\text{Sp}(1) + \frac{1}{2}\text{F}$ quotient quiver from one maximal leg. The second step, shown in Figure 15b, is the non-simple lacing of the $U(2)$ gauge node producing \mathcal{Q}_{15} .

The Coulomb branch Hilbert series may be computed exactly, but for brevity the unrefined Hilbert series is presented here as

$$\text{HS}[\mathcal{C}(\mathcal{Q}_{15})] = \frac{\left(1 + 17t^2 + 20t^3 + 117t^4 + 180t^5 + 392t^6 + 592t^7 + 701t^8 + 872t^9 + 701t^{10} + 592t^{11} + 392t^{12} + 180t^{13} + 117t^{14} + 20t^{15} + 17t^{16} + t^{18} \right)}{(1-t^2)^{18}} \quad (7.6)$$

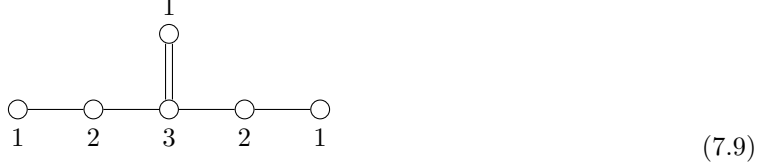
which does not elucidate the identity of this moduli space. However the Highest Weight Generating function (HWG), computed from the refined Hilbert series is given as

$$\text{HWG}[\mathcal{C}(\mathcal{Q}_{15})] = \text{PE} [\mu_1 \mu_5 t^2 + \mu_3 t^3 + \mu_2 \mu_4 t^4] \quad (7.7)$$

identifies

$$\mathcal{C}(\mathcal{Q}_{15}) = \mathbb{Z}_2 \text{ Cover } \overline{\mathcal{O}}_{[0,0,2,0,0]}^{A_5} \quad (7.8)$$

The \mathbb{Z}_2 cover is apparent in the magnetic quiver \mathcal{Q}_{15} since the difference between this quiver and the magnetic quiver for $\overline{\mathcal{O}}_{[0,0,2,0,0]}^{A_5}$, drawn in (7.9), is the non-simply laced edge of multiplicity two [43].



This result is verified with Weyl integration with the embedding of $\text{Sp}(1)$ inside E_6 with commutant $\text{SU}(6)$ decomposing the adjoint of E_6 as

$$(\mu_6)_{E_6} \rightarrow \mu_1\mu_5 + \nu^2 + \mu_3\nu \quad (7.10)$$

where the μ_i refer to $\text{SU}(6)$ highest weights fugacity and ν refers to the $\text{Sp}(1)$ highest weight fugacity. If an additional fugacity, a , for the $\text{O}(1)$ is included, the HWG of the hyper-Kähler quotient is given as

$$\text{HWG}[(\overline{\text{min.}E_6} \times \mathbb{H}) // \text{Sp}(1)] = \text{PE}[\mu_1\mu_5t^2 + a\mu_3t^3 + \mu_2\mu_4t^4] \quad (7.11)$$

which explicitly gives the construction

$$(\overline{\text{min.}E_6} \times \mathbb{H}) // \text{Sp}(1) = \mathcal{C}(\mathcal{Q}_{15}) = \mathbb{Z}_2 \text{ Cover } \overline{\mathcal{O}}_{[0,0,2,0,0]}^{A_5} \quad (7.12)$$

and as discrete quotients and hyper-Kähler quotients tend to commute, a simple corollary by gauging the \mathbb{Z}_2 in \mathbb{H} [44]

$$(\overline{\text{min.}E_6} \times \mathbb{C}^2/\mathbb{Z}_2) // \text{Sp}(1) = \overline{\mathcal{O}}_{[0,0,2,0,0]}^{A_5} \quad (7.13)$$

which is related to the duality between the $\text{Sp}(1)$ gauging of the rank-1 E_6 theory coupled to two free hypermultiplets and $\text{SU}(3)$ with six flavours [1, 19].

7.2 $(\overline{\text{min.}E_7} \times \mathbb{H}^2) // \text{Sp}(2)$

An example of the $\text{Sp}(2) + \frac{1}{2}\text{F}$ quotient quiver subtraction is performed on the affine $E_7^{(1)}$ quiver to produce \mathcal{Q}_{16} as shown in Figure 16.

The Coulomb branch Hilbert series may be computed exactly, but for brevity the unrefined Hilbert series is presented here as

$$\text{HS}[\mathcal{C}(\mathcal{Q}_{16})] = \frac{\left(\begin{aligned} &1 + 13t^2 + 16t^3 + 104t^4 + 192t^5 + 589t^6 + 1216t^7 + 2466t^8 + 4672t^9 + 7628t^{10} \\ &+ 12160t^{11} + 16970t^{12} + 22480t^{13} + 27362t^{14} + 30400t^{15} + 32006t^{16} + 30400t^{17} \\ &+ 27362t^{18} + 22480t^{19} + 16970t^{20} + 12160t^{21} + 7628t^{22} + 4672t^{23} + 2466t^{24} \\ &+ 1216t^{25} + 589t^{26} + 192t^{27} + 104t^{28} + 16t^{29} + 13t^{30} + t^{32} \end{aligned} \right)}{(1-t^2)^{11}(1-t^4)^7} \quad (7.14)$$

which does not elucidate the identity of this moduli space. Although the global symmetry is identified as $\text{SU}(2) \times \text{SO}(7)$.

This result is verified with Weyl integration with the embedding of $\text{Sp}(2)$ inside E_7 with commutant $\text{SU}(2) \times \text{SO}(7)$ decomposing the adjoint of E_7 as

$$(\mu_1)_{E_7} \rightarrow \mu_2 + \rho^2 + \nu_1^2 + \rho\mu_3\nu_1 + \mu_1\nu_2 \quad (7.15)$$

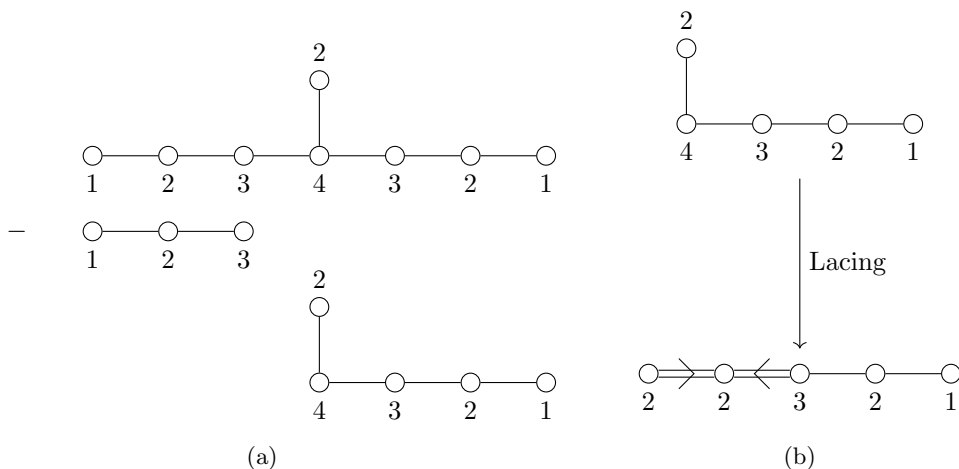


Figure 16: $\text{Sp}(2) + \frac{1}{2}\text{F}$ quotient quiver subtraction on the affine $E_7^{(1)}$ quiver which occurs in two steps. The first step is shown in Figure 16a and involves the subtraction of the $\text{Sp}(2) + \frac{1}{2}\text{F}$ quotient quiver from one maximal leg. The second step, shown in Figure 16b, is the non-simple lacing of the $\text{U}(4)$ gauge node producing \mathcal{Q}_{16} .

where the μ_i refer to B_3 highest weight fugacities, ρ refers to the A_1 highest weight fugacity, and the ν refer to $\text{Sp}(2)$ highest weight fugacities.

The conclusion is that

$$\overline{(\text{min.}E_7 \times \mathbb{H}^2)} // \text{Sp}(2) = \mathcal{C}(\mathcal{Q}_{16}) \quad (7.16)$$

8 Outlook

This paper introduces quotient quiver subtraction prescriptions for the gauging of $\text{Sp}(n)$ (coupled to a half hypermultiplet) and $\text{SO}(n)$ Coulomb branch global symmetry subgroups for $3d \mathcal{N} = 4$ quivers with unitary gauge nodes. This completes the family of prescriptions to gauging classical Coulomb branch global symmetry subgroups in unitary quivers [1, 5, 6].

There are clear future directions to explore. The first natural extension is to use Type IIB brane systems with D3, D5, and NS5 with ON planes. This would provide an algorithm on the magnetic quivers to gauge products of unitary groups in the case of ON^- , as well as give an interpretation of non-simply laced edges for the other types of ON. Secondly, it would be possible to include O3, O5, and ON which would allow for the exploration of gauging product symmetries or gauging with non-simple lacing of orthosymplectic quivers. This will all be investigated in an upcoming work.

Similarly, a natural extension is to find quotient quiver subtraction algorithms for exceptional groups. To date only G_2 gaugings of the Coulomb branch global symmetry have been constructed in unframed orthosymplectic theories [2]. It is possible that gauging G_2 Coulomb branch global symmetry subgroups may admit a simple combinatorial operation as it lies in between $\text{SO}(7)$ and $\text{SU}(3)$ in terms of Higgsing patterns for six dimensional theories.

Acknowledgments

The work of SB, AH, and GK is partially supported by STFC Consolidated Grant ST/X000575/1. The work of SB is supported by the STFC DTP research studentship grant ST/Y509231/1. The work of GK is supported by STFC DTP research studentship grant ST/X508433/1.

References

- [1] A. Hanany, R. Kalveks and G. Kumaran, *Quotient quiver subtraction*, *Nucl. Phys. B* **1009** (2024) 116731, [[2308.05853](#)].
- [2] S. Bennett, A. Hanany and G. Kumaran, *Orthosymplectic quotient quiver subtraction*, *JHEP* **12** (2024) 063, [[2409.15419](#)].
- [3] S. Bennett, A. Hanany and G. Kumaran, *Orthosymplectic Quotient Quiver Subtraction II: Framed Quivers*, [2503.19954](#).
- [4] K. A. Intriligator and N. Seiberg, *Mirror symmetry in three-dimensional gauge theories*, *Phys. Lett. B* **387** (1996) 513–519, [[hep-th/9607207](#)].
- [5] A. Hanany, R. Kalveks and G. Kumaran, *Quiver Polymerisation*, [2406.11561](#).
- [6] A. Dancer, J. F. Grimminger, J. Martens and Z. Zhong, *Complex Symplectic Contractions and 3d Mirrors*, [2406.09626](#).
- [7] N. J. Hitchin, A. Karlhede, U. Lindstrom and M. Rocek, *Hyperkahler Metrics and Supersymmetry*, *Commun. Math. Phys.* **108** (1987) 535.
- [8] A. Hanany and E. V. d. Driessche, *Higgs branch of 5d $\mathcal{N} = 1$ symplectic gauge theories and dressed instanton operators*, [2507.08669](#).
- [9] A. Hanany and E. Van den Driessche, *Chiral ring along the RG flow in 5d $\mathcal{N} = 1$* , [2510.15635](#).
- [10] S. Cremonesi, G. Ferlito, A. Hanany and N. Mekareeya, *Coulomb Branch and The Moduli Space of Instantons*, *JHEP* **12** (2014) 103, [[1408.6835](#)].
- [11] S. Cabrera, A. Hanany and M. Sperling, *Magnetic quivers, Higgs branches, and 6d $\mathcal{N}=(1,0)$ theories*, *JHEP* **06** (2019) 071, [[1904.12293](#)].
- [12] S. Cabrera, A. Hanany and M. Sperling, *Magnetic quivers, Higgs branches, and 6d $\mathcal{N} = (1, 0)$ theories — orthogonal and symplectic gauge groups*, *JHEP* **02** (2020) 184, [[1912.02773](#)].
- [13] A. Bourget, J. F. Grimminger, A. Hanany, M. Sperling, G. Zafrir and Z. Zhong, *Magnetic quivers for rank 1 theories*, *JHEP* **09** (2020) 189, [[2006.16994](#)].
- [14] A. Bourget, S. Giacomelli, J. F. Grimminger, A. Hanany, M. Sperling and Z. Zhong, *S-fold magnetic quivers*, *JHEP* **02** (2021) 054, [[2010.05889](#)].
- [15] A. Bourget, J. F. Grimminger, M. Martone and G. Zafrir, *Magnetic quivers for rank 2 theories*, *JHEP* **03** (2022) 208, [[2110.11365](#)].
- [16] C. Lawrie and L. Mansi, *The Higgs Branch of Heterotic LSTs: Hasse Diagrams and Generalized Symmetries*, [2312.05306](#).
- [17] L. Mansi and M. Sperling, *Unravelling T-Duality: Magnetic Quivers in Rank-zero Little String Theories*, [2312.12510](#).
- [18] C. Lawrie and L. Mansi, *Higgs branch of 6D $(1, 0)$ SCFTs and little string theories with Dynkin DE-type SUSY enhancement*, *Phys. Rev. D* **110** (2024) 066014, [[2406.02670](#)].

- [19] P. C. Argyres and J. R. Wittig, *Infinite coupling duals of $N=2$ gauge theories and new rank 1 superconformal field theories*, *JHEP* **01** (2008) 074, [[0712.2028](#)].
- [20] A. Hanany and E. Witten, *Type IIB superstrings, BPS monopoles, and three-dimensional gauge dynamics*, *Nucl. Phys. B* **492** (1997) 152–190, [[hep-th/9611230](#)].
- [21] A. Hanany and A. Zaffaroni, *Issues on orientifolds: On the brane construction of gauge theories with $SO(2n)$ global symmetry*, *JHEP* **07** (1999) 009, [[hep-th/9903242](#)].
- [22] B. Feng and A. Hanany, *Mirror symmetry by $O3$ planes*, *JHEP* **11** (2000) 033, [[hep-th/0004092](#)].
- [23] A. Hanany and J. Troost, *Orientifold planes, affine algebras and magnetic monopoles*, *JHEP* **08** (2001) 021, [[hep-th/0107153](#)].
- [24] S. Cremonesi, A. Hanany and A. Zaffaroni, *Monopole operators and Hilbert series of Coulomb branches of 3d $\mathcal{N} = 4$ gauge theories*, *JHEP* **01** (2014) 005, [[1309.2657](#)].
- [25] S. Cremonesi, A. Hanany, N. Mekareeya and A. Zaffaroni, *Coulomb branch Hilbert series and Hall-Littlewood polynomials*, *JHEP* **09** (2014) 178, [[1403.0585](#)].
- [26] A. Hanany and R. Kalveks, *Quiver Theories and Hilbert Series of Classical Slodowy Intersections*, *Nucl. Phys. B* **952** (2020) 114939, [[1909.12793](#)].
- [27] B. Feng, A. Hanany and Y.-H. He, *Counting gauge invariants: The Plethystic program*, *JHEP* **03** (2007) 090, [[hep-th/0701063](#)].
- [28] D. Forcella, A. Hanany, Y.-H. He and A. Zaffaroni, *The Master Space of $N=1$ Gauge Theories*, *JHEP* **08** (2008) 012, [[0801.1585](#)].
- [29] K. Gledhill and A. Hanany, *Coulomb branch global symmetry and quiver addition*, *JHEP* **12** (2021) 127, [[2109.07237](#)].
- [30] S. Cabrera and A. Hanany, *Quiver Subtractions*, *JHEP* **09** (2018) 008, [[1803.11205](#)].
- [31] A. Bourget and J. F. Grimminger, *Fibrations and Hasse diagrams for 6d SCFTs*, *JHEP* **12** (2022) 159, [[2209.15016](#)].
- [32] S. Bennett, A. Hanany, G. Kumaran, C. Li, D. Liu and M. Sperling, *Quiver subtraction on the Higgs branch*, *Nucl. Phys. B* **1016** (2025) 116917, [[2409.16356](#)].
- [33] A. Bourget, M. Sperling and Z. Zhong, *Higgs branch RG-flows via Decay and Fission*, [2401.08757](#).
- [34] K. Dasgupta and S. Mukhi, *F theory at constant coupling*, *Phys. Lett. B* **385** (1996) 125–131, [[hep-th/9606044](#)].
- [35] D. R. Morrison and C. Vafa, *Compactifications of F theory on Calabi-Yau threefolds. 1.*, *Nucl. Phys. B* **473** (1996) 74–92, [[hep-th/9602114](#)].
- [36] D. R. Morrison and C. Vafa, *Compactifications of F theory on Calabi-Yau threefolds. 2.*, *Nucl. Phys. B* **476** (1996) 437–469, [[hep-th/9603161](#)].
- [37] J. A. Minahan and D. Nemeschansky, *Superconformal fixed points with $E(n)$ global symmetry*, *Nucl. Phys. B* **489** (1997) 24–46, [[hep-th/9610076](#)].
- [38] E. Witten, *An $SU(2)$ Anomaly*, *Phys. Lett. B* **117** (1982) 324–328.
- [39] O. Chacaltana and J. Distler, *Tinkertoys for Gaiotto Duality*, *JHEP* **11** (2010) 099, [[1008.5203](#)].
- [40] A. Bourget, A. Hanany and D. Miketa, *Quiver origami: discrete gauging and folding*, *JHEP* **01** (2021) 086, [[2005.05273](#)].
- [41] K. Ohmori, Y. Tachikawa and G. Zafrir, *Compactifications of 6d $N = (1, 0)$ SCFTs with non-trivial Stiefel-Whitney classes*, *JHEP* **04** (2019) 006, [[1812.04637](#)].

- [42] R. Brylinski and B. Kostant, *Nilpotent orbits, normality, and Hamiltonian group actions*, [arXiv Mathematics e-prints](#) (Mar., 1992) [math/9204227](#), [[math/9204227](#)].
- [43] A. Hanany and A. Zajac, *Ungauging Schemes and Coulomb Branches of Non-simply Laced Quiver Theories*, *JHEP* **09** (2020) 193, [[2002.05716](#)].
- [44] S. Benvenuti, A. Hanany and N. Mekareeya, *The Hilbert Series of the One Instanton Moduli Space*, *JHEP* **06** (2010) 100, [[1005.3026](#)].